

## Bent Bonds in Benzocyclopropenes and Their Fluorinated Derivatives

O. M6,<sup>†</sup> M. Yáñez,<sup>\*†</sup> M. Eckert-Maksic,<sup>‡</sup> and Z. B. Maksic<sup>‡</sup>

Departamento de Química C-9, Universidad Autónoma de Madrid, Cantoblanco, 28049-Madrid, Spain, and Ruđer Bošković Institute, Bijenička cesta 54, 41001 Zagreb, Croatia

Received June 1, 1994 (Revised Manuscript Received November 10, 1994<sup>®</sup>)

Structure and properties of mono-, bis-, and trisannulated benzocyclopropenes and their fluorinated derivatives are studied at the MP2/6-31G\* level of theory. Particular attention is focused on bent bonding. It is shown that Mills–Nixon (MN) type of bond length alternation is apparent in fused hydrocarbons in spite of the existing bent bonds. A reversed MN effect is detected in the fluorine-substituted compounds. It appears that fluorination “freezes” that particular structure, which involves localized double bonds at coalesced (fused) positions. This conclusion is interpreted in terms of rehybridization at the carbon junction atoms and  $\pi$ -bond orders. It is supported also by topological analysis of the electronic charge density, involving calculation of  $q_c$ ,  $\nabla^2 q_c$ , and  $\epsilon$  at the bond critical points. It appears that fusion of small ring(s) affects the properties of the aromatic benzene nucleus in a chemically significant way.

### Introduction

Structural and electronic properties of planar molecules fused to small rings have attracted considerable attention recently.<sup>1–12</sup> This is not surprising since a competition between aromaticity and angular strain embodied in small annelated molecules results in new features. For example, in-plane rehybridization at the carbon junction atoms in annelated benzenes accompanied by the hyperconjugation caused by the methylene group(s) of the small carbocycles produces bond fixation within the aromatic nucleus and a substantial discrimination of  $\alpha$ - and  $\beta$ -positions toward electrophilic substituents.<sup>13</sup> This is in accordance with the original Mills–Nixon postulate<sup>14</sup> and abundant experimental evidence.<sup>15</sup> Directive property of the small fused ring in determining

a preferential site of the electrophilic attack is the so called Mills–Nixon effect in a strict sense. More generally speaking, the Mills–Nixon effect can be defined as a perturbation of the aromatic moiety by the annelated ring(s). This perturbation has some structural and electronic consequences. In particular, the annelated (ipso) bond is longer than the predetermined standard bond, whereas the adjacent (ortho) bond is shorter as a rule, if small rings are fused to the aromatic nucleus.<sup>5–10</sup> Concomitantly,  $\pi$ -density and the hybridization s-content are shifted from ipso to ortho bonds in harmony with the structural changes. This type of deformation and electron density redistribution correspond to the ordinary Mills–Nixon effect.

There are, however, situations where reversed Mills–Nixon takes place, like, e.g., in benzoborirene, benzocyclopropenyl cation,<sup>16</sup> and perfluorinated benzocyclobutenes.<sup>17</sup> On the other hand, some authors question either the very existence of the Mills–Nixon effect.<sup>18–21</sup> or claim that it is too small to be chemically relevant.<sup>22,23</sup> More specifically, the latter papers put a strong emphasis on the appearance of bent bonds, which should relieve the influence of the angular strain thus leading seemingly to very small or insignificant perturbation effects. We deemed it, therefore, worthwhile to examine bond bending in highly strained benzocyclopropenes and their fluorinated derivatives in some more detail.

<sup>†</sup> Universidad Autónoma de Madrid.

<sup>‡</sup> Ruđer Bošković Institute.

<sup>®</sup> Abstract published in *Advance ACS Abstracts*, March 1, 1995.

(1) Hiberty, P. C.; Ohanessian, G.; Delbecq, F. *J. Am. Chem. Soc.* **1985**, *107*, 3095.

(2) Stanger, A.; Vollhardt, K. P. C. *J. Org. Chem.* **1988**, *53*, 4889.

(3) Boese, R.; Bläser, D. *Angew. Chem.* **1988**, *100*, 293.

(4) Apeloig, Y.; Karni, M.; Arad, D. In NATO Advanced Research Workshop on Strain and its Implication in Organic Chemistry (NATO ASI Ser. C, **1989**, 273, 457).

(5) Eckert-Maksic, M.; Hodosek, M.; Kovacek, D.; Mitic, D.; Maksic, Z. B.; Poljanec, K. *THEOCHEM* **1990**, *206*, 89. Eckert-Maksic, M.; Hodosek, M.; Kovacek, D.; Maksic, Z. B.; Poljanec, K. *Chem. Phys. Lett.* **1990**, *171*, 49.

(6) Maksic, Z. B.; Eckert-Maksic, M.; Hodosek, M.; Koch, W.; Kovacek, D. In *Molecules in Natural Science and Medicine*; Maksic, Z. B., Eckert-Maksic, M., Eds.; Ellis Harwood: Chichester, 1991; p 333.

(7) Benassi, R.; Ianelli, S.; Nardelli, M.; Taddei, F. *J. Chem. Soc., Perkin Trans. 2* **1991**, 1381.

(8) (a) Maksic, Z. B.; Eckert-Maksic, M.; Kovacek, D.; Margetic, D. *THEOCHEM* **1992**, *260*, 241. (b) Eckert-Maksic, M.; Lesar, A.; Maksic, Z. B. *J. Chem. Soc., Perkin Trans. 2* **1992**, 993. (c) Eckert-Maksic, M.; Maksic, Z. B.; Hodosek, M.; Poljanec, K. *Int. J. Quantum Chem.* **1992**, *42*, 869.

(9) Kovacek, D.; Margetic, D.; Maksic, Z. B. *THEOCHEM* **1993**, *285*, 195. Bloor, J. E.; Eckert-Maksic, M.; Hodosek, M.; Maksic, Z. B.; Poljanec, K. *New J. Chem.* **1993**, *17*, 157.

(10) Hodosek, M.; Kovacek, D.; Maksic, Z. B. *Theor. Chim. Acta* **1993**, *86*, 343.

(11) Faust, R.; Glendening, E. D.; Streitwieser, A.; Vollhardt, K. P. C. *J. Am. Chem. Soc.* **1992**, *114*, 8263.

(12) Baldrige, K. K.; Siegel, J. S. *J. Am. Chem. Soc.* **1992**, *114*, 9583. Ou, M. C.; Chu, S. Y. *J. Phys. Chem.* **1994**, *94*, 1087.

(13) Eckert-Maksic, M.; Maksic, Z. B.; Klessinger, M. *Int. J. Quant. Chem.* **1994**, *49*, 383; *J. Chem. Soc., Perkin Trans. 2* **1994**, 285.

(14) Mills, W. H.; Nixon, I. G. *J. Chem. Soc.* **1930**, 2510.

(15) Taylor, R. *Electrophilic Aromatic Substitution*; Wiley: Chichester, 1990 and references therein.

(16) Maksic, Z. B.; Eckert-Maksic, M.; Pfeifer, K. F. *THEOCHEM* **1993**, *300*, 445.

(17) Koch, W.; Eckert-Maksic, M.; Maksic, Z. B. *Int. J. Quant. Chem.* **1993**, *48*, 319.

(18) Mitchell, R. H.; Slowey, P. D.; Kamada, T.; Williams, R. V.; Garrat, P. J. *J. Am. Chem. Soc.* **1984**, *106*, 2431.

(19) Collins, M. J.; Greedy, J. E.; Sternhell, S.; Tansey, C. W. *Austr. J. Chem.* **1990**, *43*, 1547.

(20) Thummel, R. P.; Korp, J. D.; Bernal, I.; Harlow, R. L.; Soulen, R. L. *J. Am. Chem. Soc.* **1977**, *99*, 6916. Korp, J. D.; Thummel, R. P.; Bernal, I. *Tetrahedron* **1977**, *33*, 3069.

(21) Apeloig, Y.; Arad, D.; Halton, B.; Randell, C. *J. Am. Chem. Soc.* **1986**, *108*, 4932. Apeloig, Y.; Arad, D. *J. Am. Chem. Soc.* **1986**, *108*, 3241.

(22) Stanger, A. *J. Am. Chem. Soc.* **1991**, *113*, 8277.

(23) Boese, R.; Bläser, D.; Billups, W. E.; Haley, M. M.; Maulitz, A. H.; Mahler, D. L.; Volhardt, K. P. C. *Angew. Chem., Int. Ed. Engl.* **1994**, *33*, 313.

## Methodology

The geometries of the species under investigation were optimized at the HF/6-31G\* level within the given point group symmetry. The harmonic vibrational frequencies were evaluated by using second derivative techniques in order to assure that optimized structural parameters correspond to the equilibrium geometries and to obtain the corresponding zero point energies (ZPE). Both harmonic frequencies and ZPE energies have been scaled by the empirical factor of 0.89.<sup>24</sup> The HF geometries were later refined at the MP2(full)/6-31G\* level.<sup>25</sup> Computations have been performed by employing the Gaussian 90 package of programs.<sup>26</sup>

The structural and electronic features of the investigated species are discussed in terms of the topological characteristics<sup>27-30</sup> of the electronic charge density  $\rho$ , its Laplacian  $\nabla^2\rho$ , hybridization parameters, and  $\pi$ -bond orders. This analysis is performed by locating the critical points ( $\nabla\rho(\mathbf{r}) = 0$ ) of the one-electron density distribution  $\rho(\mathbf{r})$ . These critical points can be classified<sup>28</sup> in terms of their rank (number of non-zero eigenvalues) and signature (algebraic sum of their signs) of the Hessian matrix of  $\rho(\mathbf{r})$ . Then a (3, -3) critical point will correspond to a maximum of  $\rho(\mathbf{r})$  associated with an atomic nucleus, while a (3, -1) critical point is a saddle point with two negative curvatures ( $\lambda_1, \lambda_2$ ) and a positive one ( $\lambda_3$ ). The (3, -1) critical points are of particular relevance, since they are associated with the concept of chemical bonding. A bonding interaction between two atoms is characterized by a ridge of maximum electron density (MED), usually called bond path, linking the nuclei (i.e., linking two (3, -3) critical points of  $\rho(\mathbf{r})$ ), along which the charge density is a maximum with respect to any lateral displacement (points with two negative eigenvalues). The point in which the charge density attains the minimum value along the bond path will be a (3, -1) critical point, usually called the bond critical point (bcp). It has been proved by Bader<sup>28</sup> that the local properties of  $\rho(\mathbf{r})$  at the bond critical points,  $\rho_c$  and  $\nabla^2\rho_c$ , characterize the type of atomic interactions occurring between bonded atoms. In particular, the possible  $\pi$ -character of the bond is related to its ellipticity defined as  $\epsilon = (\lambda_1/\lambda_2 - 1)$ . Useful information is also related to the so-called ring critical points, i.e., points where  $\rho$  presents two positive curvatures and a negative one. The axes associated with the two positive curvatures define a ring surface, and the density  $\rho$  is a minimum in the ring surface  $\rho_{rc}$ . The single negative curvature of  $\rho$  at a ring critical point is directed along the axis perpendicular to the ring surface. Substantial density  $\rho$  inside the three-membered ring stabilizes cyclopropane and cyclopropene moieties in spite of the large angular strain. Finally, it should be mentioned that there is a close relation between the electron density  $\rho$  at the bond critical points and the total bond order  $n$

$$n = \exp[A(\rho - B)]$$

where  $A$  and  $B$  are constants. For CC bonds in hydrocarbons one postulates  $n = 1$  in ethane implying  $B = \rho_c$  (ethane). Then

(24) Pople, J. A.; Schlegel, H. B.; Krishnan, R.; De Fries, D. J.; Binkley, J. S.; Frisch, M. J.; Whiteside, R. W.; Hout, R. F.; Hehre, W. J. *Int. J. Quantum Chem. Symp.* **1981**, *15*, 269.

(25) Hehre, W. J.; Radom, L.; Schleyer, P. v. R.; Pople, J. A. *Ab Initio Molecular Orbital Theory*; Wiley-Interscience: New York, 1986.

(26) GAUSSIAN 90, Revision I. Frisch, M. J.; Head-Gordon, M.; Trucks, G. W.; Foresman, J. B.; Schlegel, H. B.; Raghavachari, K.; Binkley, J. S.; Gonzalez, C.; Defrees, D. J.; Fox, D. J.; Whiteside, R. A.; Seeger, R.; Melius, C. F.; Baker, J.; Martin, R. L.; Kahn, L. R.; Stewart, J. J. P.; Topiol, S.; Pople, J. A. Gaussian, Inc., Pittsburgh, PA, 1990.

(27) Bader, R. F. W.; Essén, H. *J. Chem. Phys.* **1984**, *80*, 1943. Bader, R. F. W.; MacDougall, P. J.; Lau, C. D. H. *J. Am. Chem. Soc.* **1984**, *106*, 1594.

(28) Bader, R. F. W. *Atoms in Molecules. A Quantum Theory*; Oxford University Press; New York, 1990.

(29) Wiberg, K. B. *In Theoretical Models of Chemical Bonding*; Maksic, Z. B., Ed.; Springer Verlag: Berlin-Heidelberg, 1990; Part 1, p 255.

(30) Kraka, E.; Cremer, D. *In Theoretical Models of Chemical Bonding*; Maksic, Z. B., Ed.; Springer Verlag: Berlin-Heidelberg, 1990; Part 2, p 453.

$A = 6.39$  yields bond orders of 2.0 and 3.0 in ethylene and acetylene, respectively, as intuitively expected. Interestingly, the total bond order in benzene comes out to be 1.6, which is compatible with the bond order of 0.67 in Hückel theory for  $\pi$ -electrons only. Since benzene is an essential fragment in compounds examined here, it is useful to mention that ellipticities of CC bonds in benzene and ethylene are 0.230 and 0.445, respectively. In other words, ellipticity in the former molecule is half of that in ethylene as offered by the simple valence bond (VB) picture involving two Kekulé structures.

The Laplacian of the electron density ( $\nabla^2\rho(\mathbf{r})$ ) offers a complementary information to that obtained from the electron density itself, since it identifies regions of space wherein  $\rho(\mathbf{r})$  is locally concentrated ( $\nabla^2\rho < 0$ ) or depleted ( $\nabla^2\rho > 0$ ). Therefore, a negative value of  $\nabla^2\rho(\mathbf{r})$  in the internuclear region of two interacting atoms implies the formation of a typical covalent bond, since electron density is built up in that region. On the contrary, positive values of the Laplacian are characteristic of the interaction between closed shell systems where the charge is depleted from the internuclear region and concentrated on the corresponding atomic basins.

Similarly, a topological analysis of the Laplacian brings out some interesting aspects of the electronic redistribution undergone upon protonation. As we have mentioned above, a charge concentration is associated with negative values of  $\nabla^2\rho(\mathbf{r})$ , and vice versa, charge depletion is associated with positive values of  $\nabla^2\rho(\mathbf{r})$ . Accordingly, if  $\nabla^2\rho(\mathbf{r})$  in a given interatomic region becomes less negative, the chemical bond becomes activated, in the sense that the decrease in the electron density should be reflected in a smaller force constant of the bond and in a smaller dissociation energy. On the contrary, if  $\nabla^2\rho(\mathbf{r})$  becomes more negative, more charge is concentrated in the interatomic region and the bond becomes reinforced. This bond reinforcement would be mirrored in a blue shift of the corresponding stretching frequency as well as in a greater dissociation energy. The topological analysis was carried out by making use of the AIMPAC series of programs.<sup>31</sup> Finally, local  $\sigma$ -bond properties and delocalized  $\pi$ -electron densities are considered by utilizing Pauling's hybridization indices<sup>32,33</sup> and Coulson's bond orders,<sup>34</sup> respectively.

## Results and Discussion

**Bond Length and Angles.** It is common knowledge that bent bonds are the striking feature of small rings.<sup>35</sup> Interestingly, bent bonds are more rule than exceptions as shown by Wiberg and Murcko.<sup>36</sup> Appearance of bond bending has a consequence that one has to distinguish two types of bond distances: (a) interatomic bond distance (IBD) corresponding to the straight line passing through the directly linked nuclei and (b) the bond path length (BPL) defined as a ridge of maximum electron density (MED) between a pair of bonded atoms.<sup>37,38</sup> For strained rings BPL values are clearly larger than the IBD counterparts. Analogously, one can distinguish geometrical bond angles and those defined by MED lines emanating from a common nucleus. The latter are closer to the concept of the valence bond angles used in

(31) AIMPAC programs package has been provided by J. Cheeseman and R. F. W. Bader. We thank Professor Bader for this courtesy.

(32) Pauling, L. *J. Am. Chem. Soc.* **1931**, *53*, 1367.

(33) Maksic, Z. B. *In Theoretical Models of Chemical Bonding*; Maksic, Z. B., Ed.; Springer Verlag: Berlin-Heidelberg, 1990; Part 2, p 137 and references therein.

(34) McWeeny, R. *Coulson's Valence*, 3rd ed.; Oxford University Press: Oxford, 1979.

(35) Förster, Th. *Z. Phys. Chem. B* **1939**, *43*, 58. Coulson, C. A.; Moffitt, W. E. *Phil. Mag.* **1949**, *40*, 1.

(36) Wiberg, K. B.; Murcko, M. A. *THEOCHEM* **1988**, *169*, 355.

(37) Maksic, Z. B.; Eckert-Maksic, M. *Croat. Chem. Acta* **1970**, *42*, 433. Eckert-Maksic, M.; Maksic, Z. B. *THEOCHEM* **1982**, *86*, 325.

(38) Runtz, G.; Bader, R. F. W.; Messer, R. R. *Can. J. Chem.* **1977**, *55*, 3040.

(39) Wiberg, K. B.; Hadad, C. M.; LePage, T. J.; Breneman, C. M.; Frisch, M. J. *J. Phys. Chem.* **1992**, *96*, 671.

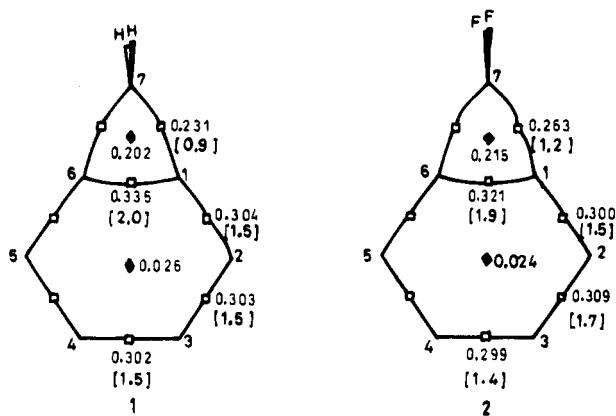


**Figure 1.** Molecular graphs of compounds **1** and **2**, showing the MP2/6-31G\* electronic charge densities (in e/au<sup>3</sup>) at the bond critical points (□) and at the ring critical points (◆), as well as the bond orders within brackets.

descriptive chemistry. The difference between these two types of bond angles yields the deviation angles of the bent bonds.

The investigated compounds are depicted in Figures 1–4. The fragment molecules cyclopropene and 3,3-difluorocyclopropene are considered for comparison. The predicted bond distances and angles are listed in Table 1. Inspection of the MED lines in Figures 1–5 reveals that bond bending is significant around the cyclopropene ring but almost negligible in bonds which do not belong to the highly strained three-membered ring. This finding casts some doubts on conjectures reached by Stanger<sup>22</sup> and Boese et al.<sup>23</sup> that the structural ring strain effect is compensated by the bent bonds and that use of the interatomic (IAD) distances in discussing the Mills–Nixon effect might be misleading. Pictorial evidence is corroborated by the actual values of IAD and BPD distances which are marginally different for all bonds of the benzene fragment, the annelated bond being an exception. It appears, therefore, that one can safely employ interatomic distances in considering bond alternation in benzene ring, since the fused bond has to be treated differently anyway, if three-membered carbocycles are annelated.<sup>8c</sup> The point is that the common bond is highly strained and considerably bent inside the aromatic ring, a feature which is absent in free benzene. Consequently, this bond is similar to and should be compared with the double bond in free cyclopropene. If the latter is taken as a standard, then annelation leads to an increase in the fused (ipso) bond distance. Nevertheless, this bond is the shortest as a rule. It is important to note, however, that the most localized  $\pi$ -bond does not necessarily correspond to the fused bond as evidenced by the calculated  $\pi$ -bond orders (vide infra). The nature of deformation induced by annelation is established conveniently by monitoring adjacent (ortho) bonds. If they are shortened, then a customary MN effect is operative. On the other hand, if adjacent bonds are stretched, then anti or reversed MN distortion takes place. Perusal of the data given in Table 1 indicates that the MN effect appears in all three parent hydrocarbons, whereas reversed MN deformation is found in the corresponding CF<sub>2</sub> derivatives. This conclusion holds irrespective of the type of bond distances (IAD or BPL) used in comparison. Changes are very small in monoannelated molecules **1** and **2** but are quite substantial in trisannelated systems **5** and **6**. Deviations of bond distances  $\Delta(\text{IAD})$  and  $\Delta$

(BPL) from the predetermined gauge values (Table 1) yield practically the same picture. Hence, bent bonds and MN or anti-MN deformations are not incompatible as some researchers seem to think. A difference between bond angles defined by straight lines and bond path angles is more pronounced. The latter are much higher in the three-membered ring assuming values close to 90°. The opposite is the case in the external angles C(2)–C(1)–C(7) which are geometrically close to 180° (e.g., in **5**). Bond path angles cannot follow such extreme deformations as they are smaller by  $\approx 20^\circ$ . This is not surprising since the carbon junction atoms possess the sp<sup>2</sup> configuration within the  $\sigma$ – $\pi$  separability approximation. The predicted structural variations can be qualitatively rationalized in terms of the bonding indices like hybridization parameters and  $\pi$ -bond orders. For that purpose we have carried out a natural bond order analysis,<sup>40,41</sup> both at the HF and MP2 levels. Values derived in this way are compatible with the classical notion of hybridization as introduced by Pauling.<sup>32</sup> The main effect upon fusion is a transfer of  $\approx 8\%$  of the s-content from the annelated bond into adjacent bonds. Consequently, the hybridization in the former bond is of the sp<sup>3</sup>–sp<sup>3</sup> (25.7%–25.7%) type. This is a very low s-content for the planar CC system belonging to the aromatic moiety, but it is still much higher than in the cyclopropane ring ( $\approx 18\%$ ). One observes that the s-character in the fused bond assumes an intermediate value between the benzene and cyclopropane hybridizations. The increase in average s-content in adjacent bonds should lead to shorter C(1)–C(2) bonds than in benzene and presumably to  $\pi$ -bond alternation in the same sense. This is indeed the case but to a very small extent in **1**. It becomes appreciable in the trisannelated compound **5**. The opposite situation occurs in fluorinated derivatives **2**, **4**, and **6** regarding annelated bonds in view of the increased hyperconjugation with CF<sub>2</sub> groups. It is also likely that the increased  $\pi$ -density shields more effectively the high positive charge of the carbon atom in CF<sub>2</sub> grouping. Both mechanisms act in the same direction leading to the reversed MN effect. The influence of fluorine substitutions on the three-membered ring is governed by rehybridization at the substituted carbon. It is well known that electronegative substituents prefer hybrids possessing high p-character placed at the directly bonded host atom.<sup>42</sup> Concomitantly, s-character is transferred to hybrids of the cyclopropene ring emanating from the C(7) atom causing substantial shortening of the C(1)–C(7) and C(6)–C(7) bonds. The increased p-character in C–F bonds leads to significant sharpening of the F–C–F angle in compounds **2**, **4**, and **6** by 6° in spite of the Coulomb repulsion between the negatively charged F atoms.

Our results (Table 1) support the hybridization model in interpreting structural properties of fluorinated hydrocarbons stating that rehybridization is the overwhelming effect as put forward first by Bennett.<sup>43</sup> This is in line with a general conclusion that (re)hybridization is the most important model of covalent bonding in organic chemistry.<sup>33</sup> It is also important to note that explicit inclusion of the correlation effects does not dramatically

(40) Foster, J. P.; Weinhold, F. *J. Am. Chem. Soc.* **1980**, *102*, 7211. Reed, A. E.; Weinhold, F. *J. Chem. Phys.* **1983**, *78*, 4066.

(41) Reed, A. E.; Weinhold, F. *J. Chem. Phys.* **1983**, *78*, 1736. Reed, A. E.; Curtiss, L. A.; Weinhold, F. *Chem. Rev.* **1988**, *88*, 899.

(42) Walsh, A. D. *Disc. Farad. Soc.* **1947**, *2*. Bent, H. A. *Chem. Rev.* **1961**, *61*, 276.

(43) Bennett, W. A. *J. Org. Chem.* **1969**, *34*, 1772.

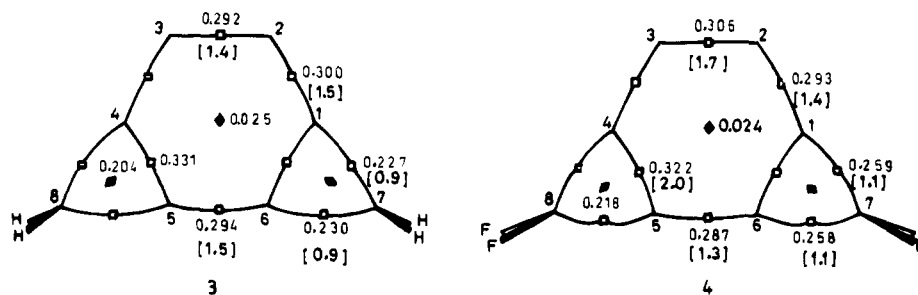


Figure 2. Molecular graphs of compounds 3 and 4. Same conventions as in Figure 1.

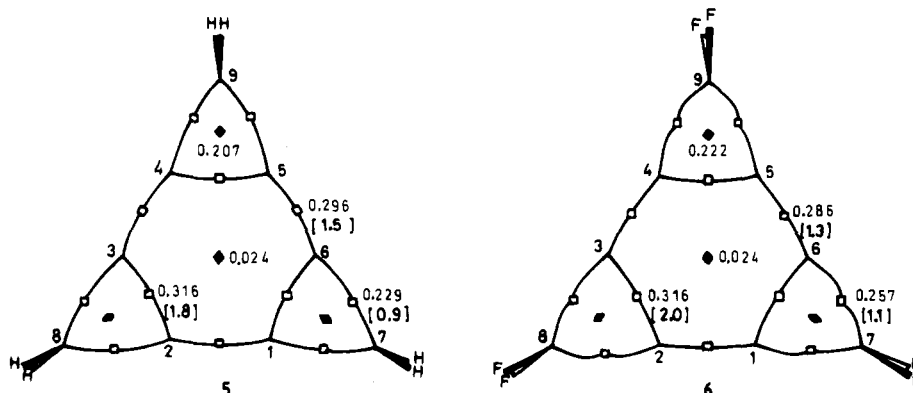


Figure 3. Molecular graphs of compounds 5 and 6. Same conventions as in Figure 1.

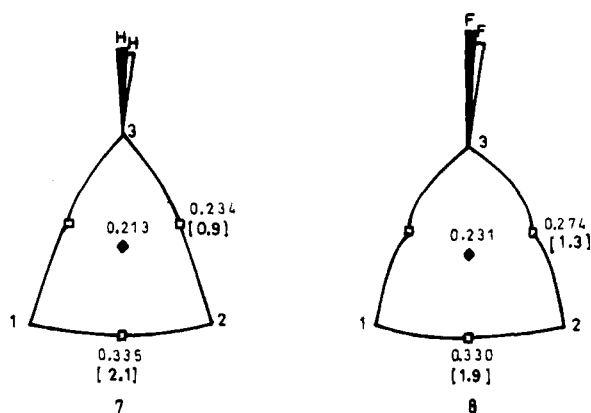


Figure 4. Molecular graphs of compounds 7 and 8. Same conventions as in Figure 1.

change bond bending.<sup>39</sup> However, in the case of the fluorinated hydrocarbons the MP2 structures are more delocalized than the HF ones.

**Topological Analysis.** As we have mentioned in previous sections, bonding characteristics can be quantitatively characterized by locating the bond and ring critical points<sup>27–30</sup> and by evaluating the Laplacian of the electronic charge density. Results of this topological analysis are summarized in Table 1 and Figures 1–4, where positions of the bond and ring critical points are indicated. Let us focus on the bonding characteristics in cyclopropene 7 and its difluoro derivative 8. Whereas the density  $\rho_c$ , for the double bonds in 7 and 8 is comparable to that found in ethylene (0.360), comparison of the bond orders (Figure 4) in these compounds reveals considerable hyperconjugation in the fluoro derivative. Relative values of  $\rho_c$  and  $\nabla^2\rho_c$  in single CC bonds in 7 and 8 are instructive. Their absolute values are considerably higher in the latter molecule reflecting increased pile-up of the electron density. This is presumably due

to rehybridization at the substituent center and transfer of the *s*-character from C–F to C(1)–C(3) bonds (vide supra). Concomitantly, ellipticity  $\epsilon$  in the C(1)–C(3) bond in 8 is lower as expected. The high anisotropy at the bond critical point in a strained bent bond is determined by the in-plane  $\pi$  nature of the curved bond path. If the participation of *p*-orbitals is diminished, then a decrease in ellipticity  $\epsilon$  follows. Ellipticity of the double bond in 8 is also smaller but for quite another reason. Here,  $\epsilon$  is dictated by the  $\pi$ -bonding which is weaker because of the hyperconjugation mentioned above. Annulation of the three-membered ring and benzene leads to substantial changes in the electron density distribution. It is useful to recall, for the sake of comparison, that the  $\rho_c$ , and  $\nabla^2\rho_c$ , for the CC bonds in benzene, are 0.310 and  $-0.845$ , respectively. Both entities are close to the free benzene values for all CC bonds in benzocyclopropene 1 with just one notable exception. The latter is given by the fused bond, where  $\rho_c$ , and  $\nabla^2\rho_c$ , are higher in absolute magnitude than in benzene. They are, however, equal to the corresponding values in free cyclopropene underlining once again that the annelated bond should be compared to the double bond in 7. Ellipticities in 1 are relatively constant for all nonannelated bonds reflecting relatively uniform  $\pi$ -electron distribution as described already by the  $\pi$ -bond orders. This is corroborated by the total bond orders  $n$  also. The fused bond has a very low ellipticity which is a result of anisotropies of the density distribution in the vicinity of the bond critical point in the plane of the ring and perpendicular to this plane. The former is a consequence of the bent bonding while the latter arises due to the  $\pi$ -bonding. It appears that the fused bonds should be compared only to the reference bond in the free cyclopropene or among themselves. The effect of difluorination in 2 is of some interest. It was recently shown<sup>44–46</sup> that bond activation (destabilization) or bond reinforcement upon substitution could be easily detected by comparison of  $\nabla^2\rho_c$  values for the substituted and for

**Table 1. Interatomic Distances (IAD), Bond Path Length (BPL), and the Corresponding Bond Angles As Calculated by the HF/6-31G\* (First Row of Each Entry) and MP2(full)/6-31G\* (Second Row of Each Entry) Methods, Respectively. Characteristic Entities  $\rho_c$ ,  $\nabla^2\rho_c$ , and  $\epsilon_c$  Are Calculated at the Bond Critical Points. The Hybridization s-Contents Were Obtained by Means of a Natural Bond Analysis (Distances in Å and Angles in Deg)<sup>a</sup>**

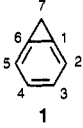
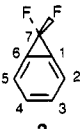

molecule	bond or angle	IAD/angle	BPL/angle	$\Delta$ (IAD)	$\Delta$ (BPL)	$\rho_c$	$\nabla^2\rho_c$	$\epsilon_c$	s-character	$\pi_{bo}$
	C(1)-C(2)	1.370	1.373	-0.016	-0.013	0.321	-0.972	0.221	43.5-33.5	0.67
		1.381	1.382	-0.014	-0.013	0.304	-0.798	0.189	43.9-33.6	
	C(2)-C(3)	1.400	1.400	0.014	0.014	0.319	-0.964	0.239	35.2-35.3	0.65
		1.407	1.407	0.012	0.012	0.303	-0.802	0.230	35.1-35.3	
	C(3)-C(4)	1.395	1.395	0.009	0.009	0.321	-0.971	0.244	35.6-35.6	0.67
		1.406	1.407	0.011	0.012	0.302	-0.800	0.225	35.5-35.5	
	C(1)-C(6)	1.332	1.343	0.056	0.051	0.361	-1.136	0.059	25.7-25.7	0.65
		1.351	1.360	0.050	0.046	0.335	-0.894	0.046	25.3-25.3	
	C(1)-C(7)	1.494	1.506	-0.001	0.001	0.240	-0.446	0.538	30.6-21.2	0.13
		1.501	1.508	-0.004	-0.004	0.231	-0.340	0.598	30.6-21.0	
	C(2)-C(1)-C(6)	124.7	121.1	4.7	1.1					
		124.5	120.5	4.5	0.5					
	C(1)-C(2)-C(3)	113.0	116.4	-7.0	-3.6					
		113.0	115.3	-7.0	-4.7					
	C(2)-C(3)-C(4)	122.3	121.9	2.3	1.9					
		122.4	121.4	2.4	1.4					
	C(1)-C(6)-C(7)	63.5	82.8	-1.2	-0.2					
		63.3	79.7	0.0	0.0					
	C(1)-C(7)-C(6)	53.0	74.6	2.5	0.3					
	53.5	70.9	0.0	0.0						
C(2)-C(1)-C(7)	173.1	153.7	28.0	17.5						
	172.2	159.7	26.6	21.6						
H-C(7)-H	113.0	116.5	0.1	0.0						
	113.1	117.6	-0.4	-0.1						
	C(1)-C(2)	1.390	1.392	0.004	0.006	0.311	-0.936	0.164	44.3-32.6	0.61
		1.390	1.391	-0.005	-0.004	0.300	-0.791	0.155	44.6-32.7	
	C(2)-C(3)	1.379	1.379	-0.007	-0.007	0.331	-1.027	0.275	35.5-35.7	0.72
		1.396	1.396	0.001	0.001	0.309	-0.833	0.240	35.5-35.6	
	C(3)-C(4)	1.416	1.416	0.030	0.030	0.310	-0.926	0.187	35.1-35.1	0.61
		1.415	1.415	0.020	0.020	0.299	-0.788	0.193	35.0-35.0	
	C(1)-C(6)	1.337	1.347	0.038	0.032	0.356	-1.080	0.106	23.3-23.3	0.69
		1.371	1.379	0.044	0.039	0.321	-0.790	0.038	22.9-22.9	
	C(1)-C(7)	1.449	1.472	0.015	0.014	0.275	-0.616	0.344	32.1-27.5	0.16
		1.455	1.472	0.010	0.010	0.263	-0.487	0.378	32.3-27.4	
	C(2)-C(1)-C(6)	124.4	120.0	4.4	0.0					
		124.1	119.2	4.1	-0.8					
	C(1)-C(2)-C(3)	113.8	115.8	-6.2	-4.2					
		113.1	115.0	-6.9	-5.0					
	C(2)-C(3)-C(4)	122.7	121.9	2.7	1.9					
		122.8	121.4	2.8	1.4					
	C(1)-C(6)-C(7)	62.5	86.3	-0.6	-1.5					
		61.9	82.8	-0.7	-2.0					
	C(1)-C(7)-C(6)	54.9	87.6	1.1	-1.6					
	56.2	84.0	1.5	-4.7						
C(2)-C(1)-C(7)	173.1	153.7	24.8	19.5						
	174.0	158.0	24.6	21.1						
F-C(7)-F	106.4	104.2	0.7	0.3						
	106.6	106.4	0.3	1.6						
	C(1)-C(2)	1.375	1.377	-0.011	-0.009	0.318	-0.944	0.228	43.8-34.2	0.68
		1.387	1.388	-0.008	-0.007	0.300	-0.769	0.188	44.2-34.1	
	C(2)-C(3)	1.416	1.416	0.030	0.030	0.308	-0.899	0.246	35.2-35.2	0.64
		1.423	1.423	0.028	0.028	0.292	-0.742	0.239	35.2-35.2	
	C(5)-C(6)	1.360	1.366	-0.026	-0.020	0.311	-0.869	0.189	42.1-42.1	0.67
		1.372	1.375	-0.023	-0.020	0.294	-0.705	0.139	42.4-42.4	
	C(1)-C(6)	1.341	1.352	0.065	0.060	0.356	-1.107	0.071	25.3-25.6	0.64
		1.359	1.369	0.058	0.055	0.331	-0.865	0.061	25.0-25.1	
	C(1)-C(7)	1.501	1.513	0.006	0.008	0.237	-0.436	0.526	30.4-21.2	0.13
		1.509	1.516	0.004	0.004	0.227	-0.328	0.590	30.5-21.0	
	C(6)-C(7)	1.493	1.507	-0.002	0.002	0.240	-0.456	0.484	32.4-21.1	
		1.501	1.509	-0.004	-0.003	0.230	-0.344	0.537	32.4-20.8	
	C(2)-C(1)-C(6)	126.2	121.8	6.2	1.8					
		125.9	121.1	5.9	1.1					
	C(1)-C(2)-C(3)	115.9	117.9	-4.1	-2.1					
		116.1	117.0	-3.9	-3.0					
	C(1)-C(6)-C(5)	117.9	115.5	-2.1	-4.5					
		117.9	114.2	-2.1	-5.8					
	C(1)-C(6)-C(7)	63.7	85.5	-1.0	2.5					
	63.5	82.2	0.2	2.5						
C(6)-C(1)-C(7)	63.1	82.6	-1.6	-0.4						
	62.8	79.4	-0.5	-0.3						
C(1)-C(7)-C(6)	53.2	74.8	2.7	0.5						
	53.7	71.2	0.2	0.3						
C(2)-C(1)-C(7)	170.7	155.6	25.6	19.4						
	171.2	159.4	25.6	21.3						
C(5)-C(6)-C(7)	178.4	159.0	33.3	22.8						
	178.6	163.6	33.0	25.5						
H-C(7)-H	113.1	116.6	0.2	0.1						
	113.1	117.7	-0.4	0.0						

Table 1 (Continued)

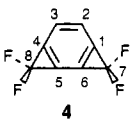
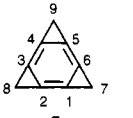
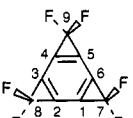
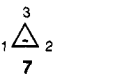
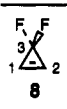
molecule	bond or angle	IAD/angle	BPL/angle	$\Delta(\text{IAD})$	$\Delta(\text{BPL})$	$q_c$	$\nabla^2 q_c$	$\epsilon_c$	s-character	$\pi_{bo}$
 4	C(1)-C(2)	1.413	1.415	0.027	0.029	0.030	-0.878	0.128	44.1-32.8	0.57
		1.405	1.405	0.010	0.010	0.293	-0.756	0.132	44.4-32.9	
	C(2)-C(3)	1.376	1.376	-0.010	-0.010	0.332	-1.023	0.309	35.9-35.9	0.75
		1.401	1.401	0.006	0.006	0.306	-0.808	0.255	35.8-35.8	
	C(5)-C(6)	1.395	1.401	0.009	0.015	0.294	-0.822	0.090	42.3-42.3	0.56
		1.389	1.392	-0.006	-0.003	0.287	-0.703	0.082	42.6-42.6	
	C(1)-C(6)	1.332	1.343	0.033	0.028	0.362	-1.109	0.150	23.4-24.1	0.74
		1.372	1.380	0.045	0.040	0.322	-0.792	0.065	22.9-23.6	
	C(1)-C(7)	1.455	1.478	0.021	0.020	0.272	-0.601	0.343	31.6-27.4	0.15
		1.465	1.481	0.020	0.019	0.259	-0.471	0.379	31.7-27.3	
	C(6)-C(7)	1.450	1.476	0.016	0.018	0.272	-0.606	0.328	34.0-26.8	
		1.461	1.479	0.016	0.017	0.258	-0.470	0.367	34.2-26.7	
	C(2)-C(1)-C(6)	126.9	121.3	6.9	1.3					
		126.5	120.6	6.5	0.6					
	C(1)-C(2)-C(3)	115.9	117.2	-4.1	-2.8					
		116.6	116.3	-3.4	-3.7					
	C(1)-C(6)-C(5)	117.2	113.9	-2.8	-6.1					
		117.2	112.7	-2.8	-7.3					
	C(1)-C(6)-C(7)	62.9	89.3	-0.2	1.5					
	62.2	85.1	-0.4	0.3						
C(6)-C(1)-C(7)	62.5	87.0	-0.6	-0.8						
	61.9	83.1	-0.7	-1.7						
C(1)-C(7)-C(6)	54.5	86.2	0.7	-3.0						
	55.9	82.8	1.2	-2.5						
C(2)-C(1)-C(7)	170.6	151.7	22.3	17.5						
	171.6	156.3	22.2	19.4						
C(5)-C(6)-C(7)	179.9	156.8	31.6	22.6						
	179.4	162.2	30.0	25.3						
F-C(7)-F	106.8	104.7	1.1	0.8						
	107.3	107.2	1.6	2.4						
 5	C(1)-C(2)	1.356	1.360	-0.030	-0.026	0.313	-0.869	0.193	42.8-42.8	0.70
		1.367	1.370	-0.028	-0.025	0.296	-0.705	0.127	43.2-43.2	
	C(1)-C(6)	1.359	1.370	0.083	0.078	0.343	-1.015	0.060	24.8-24.8	0.61
		1.377	1.387	0.076	0.073	0.316	-0.770	0.051	24.4-24.4	
	C(1)-C(7)	1.497	1.511	0.002	0.006	0.239	-0.458	0.458	32.2-21.2	0.13
		1.505	1.514	0.000	0.002	0.229	-0.347	0.501	32.2-20.9	
	C(2)-C(1)-C(6)	120.0	116.5	0.0	-3.5					
		120.0	115.2	0.0	-4.8					
	C(1)-C(6)-C(7)	63.0	85.0	-1.7	2.0					
		62.8	81.7	-0.5	2.0					
	C(1)-C(7)-C(6)	54.0	76.0	3.5	1.7					
		54.4	72.7	0.9	1.8					
	C(2)-C(1)-C(7)	177.0	157.5	31.9	21.3					
	177.2	163.1	31.6	25.0						
H-C(7)-H	113.2	116.7	0.3	0.2						
	113.2	117.8	-0.3	0.1						
 6	C(1)-C(2)	1.408	1.413	0.022	0.027	0.289	-0.802	0.063	42.5-42.5	0.54
		1.394	1.397	-0.001	0.002	0.286	-0.697	0.060	42.8-42.8	
	C(1)-C(6)	1.332	1.344	0.033	0.029	0.361	-1.092	0.172	23.7-23.7	0.76
		1.380	1.389	0.053	0.049	0.316	-0.748	0.072	23.2-23.2	
	C(1)-C(7)	1.456	1.480	0.022	0.022	0.271	-0.603	0.320	33.5-26.7	0.15
		1.468	1.485	0.023	0.023	0.257	-0.471	0.353	33.7-26.6	
	C(2)-C(1)-C(6)	120.0	115.7	0.0	-4.3					
		120.0	114.7	0.0	-5.3					
	C(1)-C(6)-C(7)	63.8	89.4	0.7	1.6					
		62.0	84.9	-0.6	0.1					
	C(1)-C(7)-C(6)	54.4	85.6	0.6	-3.6					
		56.0	82.6	1.3	-2.7					
	C(2)-C(1)-C(7)	176.2	154.9	27.9	20.7					
	178.0	160.4	30.0	22.1						
F-C(7)-F	107.3	105.3	1.6	1.4						
	107.9	108.0	1.8	1.4						
 7	C(1)-C(2)	1.276	1.292	0	0	0.370	-1.100	0.304	35.6-35.6	0.99
		1.301	1.314	0	0	0.335	-0.894	0.350	35.5-35.5	
	C(1)-C(3)	1.495	1.505	0	0	0.244	-0.429	0.606	24.8-20.6	0.13
		1.505	1.512	0	0	0.234	-0.332	0.646	24.8-20.2	
	H-C-H	112.9	116.5							
		113.5	117.7							
	H-C(1)-C(2)	150.2	140.8							
		150.0	141.2							
	C(1)-C(2)-C(3)	64.7	83.0	0	0					
		63.3	79.7	0	0					
	C(1)-C(3)-C(2)	50.5	74.3	0	0					
		53.5	70.9	0	0					
	H-C(1)-C(3)	145.1	136.2	0	0					
	145.6	138.1	0	0						

Table 1 (Continued)

molecule	bond or angle	IAD/angle	BPL/angle	$\Delta(\text{IAD})$	$\Delta(\text{BPL})$	$\rho_c$	$\nabla^2\rho_c$	$\epsilon_c$	s-character	$\pi_{bo}$
	C(1)–C(2)	1.299	1.315	0	0	0.356	–1.016	0.270	32.1–32.1	0.98
		1.327	1.340	0	0	0.330	–0.791	0.172	31.9–31.9	
	C(1)–C(3)	1.434	1.458	0	0	0.288	–0.671	0.272	27.0–27.1	0.18
		1.445	1.462	0	0	0.274	–0.532	0.309	26.8–27.2	
	F–C–F	105.7	103.9							
		106.1	104.8							
	H–C(1)–C(2)	148.5	138.0							
		148.0	138.3							
	C(1)–C(2)–C(3)	63.1	87.8	0	0					
		62.6	84.8	0	0					
	C(1)–C(3)–C(2)	53.8	89.2	0	0					
		54.7	85.3	0	0					
H–C(1)–C(3)	148.3	134.2	0	0						
	149.4	136.9	0	0						

<sup>a</sup> Relative differences of IAD and BPL distances (angles) for all bonds belonging to the three-membered ring are determined by taking the corresponding values in **7** and **8** as standards. A value of the CC IAD bond distance in free benzene of 1.395 Å (MP2/6-31G<sup>\*\*</sup>) is chosen as a gauge for the remaining CC bond benzocyclopropanes. Topological indices  $\rho_c$ ,  $\nabla^2\rho_c$ , and  $\epsilon_c$  in benzene are 0.310, –0.845, and 0.218, respectively.

the unsubstituted molecules. As we mentioned above, bond activations are accompanied by a decrease in the absolute value of  $\nabla^2\rho_c$ , whereas more negative values of the Laplacian implies higher concentrations of the electron density between the bonded nuclei leading ultimately to reinforcement of the bond strength. It is apparent by comparing the Laplacian maps of compounds **1** and **2** (Figure 5a,b) that fluorine substitution leads to strengthening of the apical C(1)–C(7) and C(6)–C(7) bonds which is manifested in shifting the corresponding stretching frequency to higher values (vide infra). In contrast, adjacent and distal bonds of the benzene ring are weakened, thus making them somewhat more susceptible to rupture. This is substantiated by the low absolute magnitudes of  $\rho_c$  and  $\nabla^2\rho_c$ . These changes are not highly pronounced, however. It is interesting to observe that lower ellipticities are compatible with smaller  $\pi$ -bond orders if the corresponding bonds are taken into account. The same holds for higher ellipticities and stronger  $\pi$ -electron bond fixation. A close scrutiny of the topological parameters in **3** and **4** reveals that bonds which are weaker in one molecule are stronger in the other and vice versa. This is in harmony with a general picture that fluorination “freezes” a Kekulé structure, which is complementary to that found in a pure hydrocarbon. A similar conclusion is drawn by examining critical points in **5** and **6**. The annelated bonds are stronger in the latter (perfluoro) compound as compared to the unsubstituted hydrocarbon **5**. The opposite is true for adjacent bonds. It follows that  $\pi$ -bond fixation is transferred from adjacent to fused bonds upon fluorination, which is corroborated by the calculated  $\pi$ -bond orders and ellipticities. This is also evidenced by changes in the topological total bond orders  $n$  (Figures 1–4).

In concluding this section, it is worth mentioning that density at the three-membered ring critical points,  $\rho_{cr}$ , is greater in fluorinated derivatives, which is indicative of a more pronounced surface  $\sigma$ -aromaticity.<sup>30</sup> This is an additional reason why cyclopropene fragments are more stable in perfluoro compounds compared to hydrocarbons. We note in passing that  $\rho_{cr}$  in the benzene moiety assumes a very low value of 0.02–0.03 in the series 1–6.

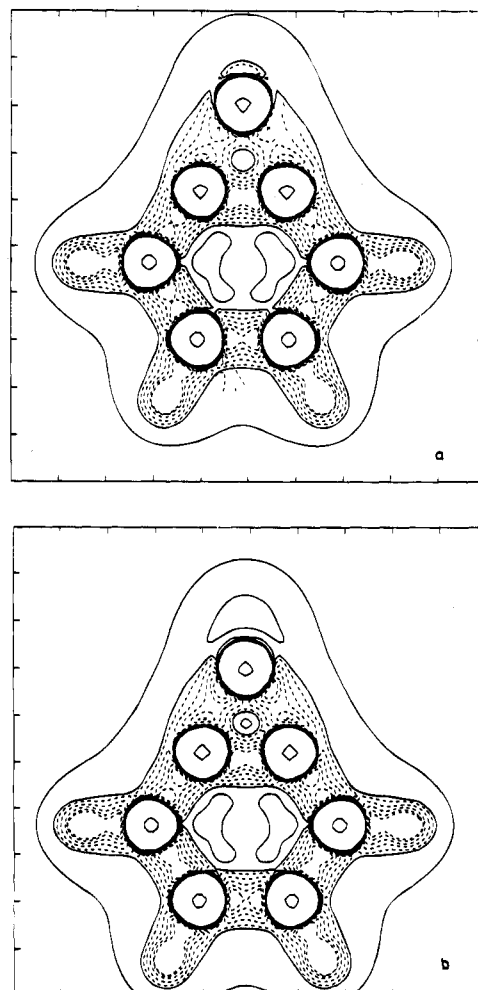


**Figure 5.** Contour maps of the Laplacian of the charge density of compounds (a) **1** and (b) **2**. Positive values of  $\nabla^2\rho_c$  are denoted by solid lines and negative values by dashed lines. Contour values in au are  $\pm 0.05$ ,  $\pm 0.25$ ,  $\pm 0.50$ ,  $\pm 0.75$ , and  $\pm 0.95$ .

**Energetic and Vibrational Features.** The total energies of the compounds under investigation, the corresponding zero point energies (ZPE), and the dipole moments have been summarized in Table 2. Tables 3–5 present the harmonic vibrational frequencies of compounds 1–6. For the sake of a better comparison, each unsubstituted compound and its corresponding fluorine

(44) Alcamí, M.; Mó, O.; Yañez, M.; Abboud, J. L. M.; Elguero, J. *Chem. Phys. Lett.* **1990**, *172*, 471.

(45) Alcamí, M.; Mó, O.; Yañez, M.; Abboud, J. L. M. *J. Phys. Org. Chem.* **1990**, *4*, 177.

(46) Abboud, J. L. M.; Cañada, T.; Homan, H.; Notario, R.; Cativiela, C.; Diaz de Villegas, M. D.; Bordejé, M. C.; Mó, O.; Yañez, M. *J. Am. Chem. Soc.* **1992**, *114*, 4728.

**Table 2. MP2/6-31G\* Total Energies (Hartrees), Zero Point Energies<sup>a</sup> (kcal/mol), and Dipole Moments (D)**

compd	<i>E</i>	ZPE	$\mu$
1	-269.38827	62.8	0.08
2	-467.44379	53.9	1.39
3	-307.28220	65.6	0.08
4	-703.39051	47.6	1.30
5	-345.17793	68.4	0.0
6	-939.33391	41.4	0.0

<sup>a</sup> Evaluated at the HF/6-31G\* level and scaled by the empirical factor 0.89.

**Table 3. Harmonic Vibrational Frequencies (cm<sup>-1</sup>) of Compounds 1 and 2**

compd 1	compd 2
3016(a <sub>1</sub> ) {C5-H, C2-H stret ip + C4H, C3H stret ip}ip	3031(a <sub>1</sub> )
3011(b <sub>2</sub> ) {C5H, C2H stret op + C4H, C3H stret op}ip	3030(b <sub>2</sub> )
2997(a <sub>1</sub> ) {C5H, C2H stret ip + C4H, C3H stret ip}op	3007(a <sub>1</sub> )
2983(b <sub>2</sub> ) {C5H, C2H stret op + C4H, C3H stret op}op	2992(b <sub>2</sub> )
2951(b <sub>1</sub> ) C7H <sub>2</sub> stret asym	
2890(a <sub>1</sub> ) C7H <sub>2</sub> stret asym	
1676(a <sub>1</sub> ) C1-C6 + C4-C3 stret ip	1666(a <sub>1</sub> )
1574(b <sub>2</sub> ) C5-C4 + C2-C3 stret op	1588(b <sub>2</sub> )
1469(a <sub>1</sub> ) C7H <sub>2</sub> rocking	
1441(b <sub>2</sub> ) C4H + C3H bend ip	1456(b <sub>2</sub> )
1422(a <sub>1</sub> ) C5H + C2H bend ip	1422(a <sub>1</sub> )
1285(a <sub>1</sub> ) C7C6C1 stret	1322(a <sub>1</sub> )
1262(b <sub>2</sub> ) C5H, C2H + C4H, C3H bend ip	1277(b <sub>2</sub> )
1124(a <sub>1</sub> ) C5H, C2H + C4H, C3H bend op	1220(a <sub>1</sub> )
	1152(b <sub>1</sub> ) C7F <sub>2</sub>
1091(b <sub>2</sub> ) C7H <sub>2</sub> wag.	asym stret
1083(b <sub>2</sub> ) C5H, C2H + C4H, C3H bend op	1113(b <sub>2</sub> )
1067(a <sub>1</sub> ) C4-C3 + C6-C1 stret op	1107(a <sub>1</sub> )
1006(b <sub>1</sub> ) C7H <sub>2</sub> rocking	
976(b <sub>2</sub> ) ring def (C6C5C4 + C1C2C3 bend op)	996(b <sub>2</sub> )
956(a <sub>1</sub> ) ring breathing	1019(a <sub>1</sub> )
928(b <sub>1</sub> ) C5, C2 + C4, C3 pyramid. op	966(b <sub>1</sub> )
827(a <sub>1</sub> ) C5, C4 + C2, C3 stret ip	962(a <sub>1</sub> )
744(b <sub>1</sub> ) C5, C2 + C4, C3 pyramid. ip	752(b <sub>1</sub> )
654(b <sub>2</sub> ) ring def	796(b <sub>2</sub> )
	714(a <sub>1</sub> ) C7F <sub>2</sub>
558(a <sub>1</sub> ) ring def (C6, C5, C4 + C1, C2, C3 bend. ip)	sym stret
425(b <sub>2</sub> ) ring def (C6, C5, C4, C3 bend.)	577(a <sub>1</sub> )
	625(b <sub>2</sub> )
	475(b <sub>1</sub> ) C7F <sub>2</sub>
	sym stret
	383(a <sub>1</sub> ) C7F <sub>2</sub>
	siccors
344(b <sub>1</sub> ) ring puckering	352(b <sub>1</sub> )
	275(b <sub>2</sub> ) C7F <sub>2</sub>
	wag.
191(b <sub>1</sub> ) C7H <sub>2</sub> bend. out of plane	
	99(b <sub>1</sub> ) C7F <sub>2</sub>
	rocking

<sup>a</sup> ip and op stand for in phase and out of phase, respectively.

derivative are presented in the same table. Compounds **1** and **2** belong to the  $C_{2v}$  symmetry point group; hence, five of their vibrational modes (those which belong to the  $a_2$  irreducible representation) are IR inactive. Therefore, only the 28 remaining vibrations have been collected in Table 2. Something similar can be said of compounds **3** and **4**, which belong also to the  $C_{2v}$  symmetry point group and present seven inactive vibrational modes. Species **5** and **6** belong to the  $D_{3h}$  symmetry group. Therefore, from their 39 normal vibrational modes only 11 (those of  $a_2$  and  $e'$  symmetry) are active in IR. There are several common features regarding the harmonic vibrations of these species. It can be observed, for instance, that fluorine substitution causes a slight blue shift of the C-H stretching frequencies. This is consistent, as we have seen earlier, with the slight increase of the electronic charge densities at the corresponding bond critical points. A similar effect is observed regarding the C-C stretching frequencies of the carbon atoms which pertain to the three-membered ring. Again, this finding is consistent

**Table 4. Harmonic Vibrational Frequencies (cm<sup>-1</sup>) of Compounds 3 and 4**

compd 3	comp 4
3015(a <sub>1</sub> ) CH stret ip	3040(a <sub>1</sub> )
2999(b <sub>2</sub> ) CH stret op	3025(b <sub>2</sub> )
2956(b <sub>1</sub> ) CH <sub>2</sub> asym stret ip	
2893(a <sub>1</sub> ) CH <sub>2</sub> sym stret ip	
2892(b <sub>2</sub> ) CH <sub>2</sub> sym stret op	
1672(b <sub>2</sub> ) C1-C6 + C4-C5 stret op	1673(b <sub>2</sub> )
1628(a <sub>1</sub> ) C2-C3 + C5-C6 stret ip	1628(a <sub>1</sub> )
1467(a <sub>1</sub> ) CH <sub>2</sub> siccors ip	
1465(b <sub>2</sub> ) CH <sub>2</sub> siccors op	
1393(a <sub>1</sub> ) C2, C3 + C5, C6 stret op	1430(a <sub>1</sub> )
1389(b <sub>2</sub> ) CH bend.	1395(b <sub>2</sub> )
1344(a <sub>1</sub> ) three-membered ring stret ip	1384(a <sub>1</sub> )
	1273(b <sub>2</sub> ) CF <sub>2</sub> sym stret op
	1252(a <sub>1</sub> ) CF <sub>2</sub> sym stret ip
1154(b <sub>2</sub> ) CH bend. ip	1187(b <sub>2</sub> )
	1169(b <sub>1</sub> ) CF <sub>2</sub> bend. out of plane
	1101(a <sub>1</sub> )
1118(a <sub>1</sub> ) CH bend. op	
1100(a <sub>1</sub> ) CH <sub>2</sub> wag. ip	
1091(b <sub>2</sub> ) CH <sub>2</sub> wag. op	
1017(b <sub>2</sub> ) CH <sub>2</sub> wag. op	
1014(b <sub>1</sub> ) CH <sub>2</sub> twist. ip	
985(a <sub>1</sub> ) ring breathing	1036(a <sub>1</sub> )
983(b <sub>1</sub> ) CH <sub>2</sub> rocking op	
972(b <sub>2</sub> ) ring def (C3, C4, C5 + C2, C1, C6 bend. op)	999(b <sub>2</sub> )
	830(b <sub>2</sub> ) CF <sub>2</sub> sym stret op
816(b <sub>1</sub> ) CH bend. out of plane	825(b <sub>1</sub> )
750(a <sub>1</sub> ) ring def (C3, C4, C5 + C2, C1, C6 bend. ip)	605(a <sub>1</sub> )
612(a <sub>1</sub> ) ring def (C3, C4, C5 + C2, C1, C6 bend. ip)	633(a <sub>1</sub> )
565(b <sub>2</sub> ) ring def (C7, C8 bend. op)	725(b <sub>2</sub> )
	571(b <sub>2</sub> ) CF <sub>2</sub> siccors
	465(b <sub>1</sub> ) CF <sub>2</sub> asym stret ip
	410(b <sub>2</sub> )
469(b <sub>2</sub> ) ring def	567(b <sub>1</sub> )
429(b <sub>1</sub> ) ring puckering	798(a <sub>1</sub> ) CF <sub>2</sub> rocking
371(a <sub>1</sub> ) ring def (C7, C8 bend. ip)	348(a <sub>1</sub> ) CF <sub>2</sub> wag. ip
	341(b <sub>2</sub> ) CF <sub>2</sub> wag. op
	200(b <sub>1</sub> ) CF <sub>2</sub> twisting
149(b <sub>1</sub> ) CH <sub>2</sub> bend. out of plane	
	174(a <sub>1</sub> ) CF <sub>2</sub> wag. ip
	60(b <sub>1</sub> ) CF <sub>2</sub> rocking

<sup>a</sup> ip and op stand for in phase and out of phase, respectively.

**Table 5. Harmonic Vibrational Frequencies (cm<sup>-1</sup>) of Compounds 5 and 6**

compd 5	compd 6
2960(a <sub>2</sub> '') CH <sub>2</sub> asym stret ip	
2895(e') CH <sub>2</sub> sym stret op	
1676(e') C5-C6 + C3-C4 stret ip	1665(e')
1463(e') CH <sub>2</sub> sym stret op	
1320(e') C1-C6 + C3-C2 stret op	1376(e')
1105(e') CH <sub>2</sub> wag. op	
1000(e') three-membered ring stret op	1276(e')
964(a <sub>2</sub> '') C7, C8, C9 bend. out of plane ip	1186(a <sub>2</sub> '')
	859(e') CF <sub>2</sub> sym stret op
	741(e') CF <sub>2</sub> sym stret ip
585(e') C6, C1, C2 + C3, C4, C5 bend. ip	588(e')
374(e') ring def (C7, C8, C9 bend.)	460(a <sub>2</sub> '') CF <sub>2</sub> bend.
	409(e')
	159(e') CF <sub>2</sub> wag.
109(a <sub>2</sub> '') CH <sub>2</sub> rocking	
	39(a <sub>2</sub> '') CF <sub>2</sub> rocking

<sup>a</sup> ip and op stand for in phase and out of phase, respectively.

with the reinforcement of these bonds upon fluorine substitution, as shown both by the Laplacians and the values of  $\rho$  at the bond critical points. Interestingly, the C-F stretching frequencies of compounds **2** and **4** are predicted to appear in the 1100–1200 cm<sup>-1</sup> range in agreement with the general behavior of the majority of



carbon-fluorine compounds.<sup>47</sup> It may be also noticed that the topological analysis of these bonds reveals that the C-F linkages of species **4** should be slightly stronger than those of **2** again in agreement with the estimated values of their stretching frequencies. The corresponding frequencies of species **6** are found at much lower values, because, due to the symmetry of this system, the combinations of the asymmetric stretchings which are predicted at 1286 cm<sup>-1</sup> are IR inactive. It may be observed, however, that the asymmetric stretchings follow the same sequence as the electronic charge densities at the C-F bond critical points.

### Conclusion

We have shown that BLP distances, taken along the ridge of the maximum electron density between two linked atoms, alternate in the Mills-Nixon sense in benzocycloalkenes **1**, **3**, and **5**. On the other hand, anti-MN alternation is found in fluoro derivatives **2**, **4**, and **6**. It appears that  $\pi$ -bond fixation occurs in the annelated

bonds in the latter compounds. To put it in another way, the Kekulé structure involving double bonds placed on the common fused bonds becomes more favorable upon fluorination. This conjecture is supported by the topological analysis as evidenced by calculated parameters  $\rho_c$ ,  $\nabla^2\rho_c$  and  $\epsilon$  at the bond critical points in question. It follows, as a corollary, that appearance of bent bonds does not cancel out either the MN or reversed MN effect. Importance of cyclopropene as a gauge in providing the standard double bond, which serves as a vantage point for measuring changes induced by annelation, is stressed in this respect. To summarize in a single sentence: Fusion of small rings to benzene nucleus affects properties of the latter in a way which has significant chemical consequences.<sup>13,48</sup> In particular, annelation of a small ring has a decisive influence on the regioselectivity in the electrophilic substitution reactions.

**Acknowledgment.** This work has been partially supported by the DGICYT Project No. PB93-0289-C02-01.

JO9409039

(47) Hudlicky, M. *Organic Fluorine Chemistry*; Plenum Press: New York, 1971.

(48) Martínez, A.; Jimeno, M. L.; Elguero, J.; Fruchier, A. *New J. Chem.* **1994**, *18*, 269.